

## Universal Exchange-Driven Phonon Splitting in Antiferromagnets

Ch. Kant,<sup>1</sup> M. Schmidt,<sup>1</sup> Zhe Wang,<sup>1</sup> F. Mayr,<sup>1</sup> V. Tsurkan,<sup>1,2</sup> J. Deisenhofer,<sup>1,\*</sup> and A. Loidl<sup>1</sup>

<sup>1</sup>Experimental Physics V, Center for Electronic Correlations and Magnetism, University of Augsburg, 86135 Augsburg, Germany

<sup>2</sup>Institute of Applied Physics, Academy of Sciences of Moldova, MD-2028 Chişinău, Republic of Moldova

(Received 22 July 2011; published 26 April 2012)

We report a linear dependence of the phonon splitting  $\Delta\omega$  on the nondominant exchange coupling constant  $J_{\text{nd}}$  in the antiferromagnetic transition-metal monoxides MnO, FeO, CoO, NiO, and in the frustrated antiferromagnetic oxide spinels  $\text{CdCr}_2\text{O}_4$ ,  $\text{MgCr}_2\text{O}_4$ , and  $\text{ZnCr}_2\text{O}_4$ . It directly confirms the theoretical prediction of an exchange-induced splitting of the zone-center optical phonon for the monoxides and explains the magnitude and the change of sign of the phonon splitting on changing the sign of the nondominant exchange also in the frustrated oxide spinels. The experimentally found linear relation  $\hbar\Delta\omega = \beta J_{\text{nd}} S^2$  with slope  $\beta = 3.7$  describes the splitting for both systems and agrees with the observations in the antiferromagnets  $\text{KCoF}_3$  and  $\text{KNiF}_3$  with perovskite structure and negligible next-nearest neighbor coupling. The common behavior found for very different classes of cubic antiferromagnets suggests a universal dependence of the exchange-induced phonon splitting at the antiferromagnetic transition on the nondominant exchange coupling.

DOI: 10.1103/PhysRevLett.108.177203

PACS numbers: 75.50.Ee, 75.25.-j, 75.30.Et, 78.30.Am

The interplay of magnetism and the underlying crystal lattice is a topical issue of condensed-matter physics. This spin-phonon coupling can relieve frustration via a spin-driven Jahn-Teller effect in frustrated magnets [1,2], lead to novel excitations such as electromagnons in multiferroics [3,4], and can even bear the potential for future applications via magnetodielectric effects [5]. For transition-metal monoxides (TMMOs) a magnetism-induced anisotropy in the lattice response was predicted theoretically [6]. This approach has been extended to other material classes such as Cr based spinels, which are hallmark systems for highly frustrated magnets [7–10], where spin-phonon coupling leads to a splitting of characteristic phonon modes [11–15].

TMMOs are both textbook examples for antiferromagnets governed by superexchange in a cubic rock-salt lattice and benchmark materials for the understanding of strongly correlated electronic systems [16,17]. The magnetic structure of the TMMOs consists of ferromagnetic planes coupled antiferromagnetically, e.g., along [111] as depicted in Fig. 1(a). The antiferromagnetic 180° next-nearest-neighbor (nnn) exchange  $J_2$  is supposed to be the driving force of the magnetic ordering [18,19], leaving the nearest-neighbor (nn) exchange  $J_1$  frustrated, since it cannot satisfy all its pairwise interactions [see Fig. 1(c)]. In Fig. 1(d) we plot the Néel temperatures of the TMMOs (MnO:  $T_N = 118$  K [20],  $\text{Fe}_{0.92}\text{O}$ :  $T_N \approx 198$  K [21,22], CoO:  $T_N = 289$  K [23,24], and NiO:  $T_N = 523$  K [25]) as a function of  $J_2 S(S+1)$ , using  $J_2$  values from [26], and find a linear slope of  $k_B T_N / J_2 S(S+1) \sim 3$  (solid line) close to the expected relation in mean-field approximation (dashed line). In a pioneering paper Massidda *et al.* [6] showed that even for purely cubic TMMOs the antiferromagnetic order is accompanied by a Born-effective-charge redistribution from spherical to

cylindrical with the antiferromagnetic axis being the symmetry axis, e.g. [111]. Consequently, the cubic zone-center optical phonon is predicted to split into two phonon modes with eigenfrequencies  $\omega_{\parallel}$  and  $\omega_{\perp}$  for light polarized parallel and perpendicular to the cylindrical axis, respectively [see Fig. 1(b)]. The pure lattice contributions due to

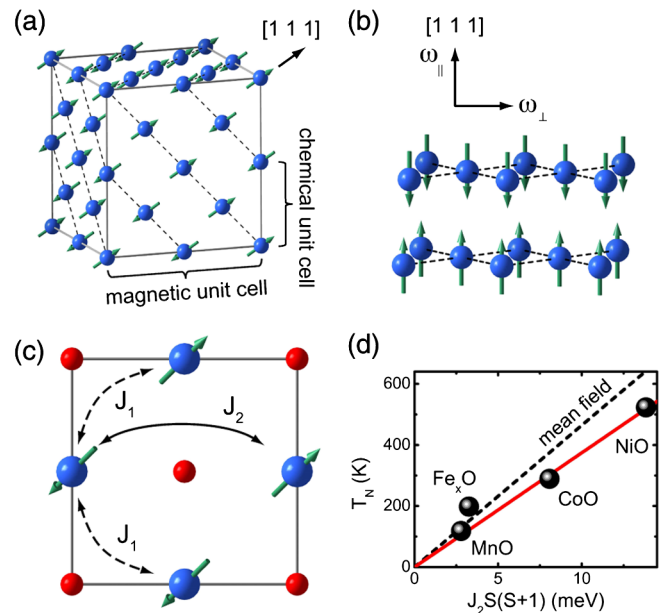


FIG. 1 (color online). Magnetic properties of the investigated TMMOs. (a) Magnetic unit cell showing the antiferromagnetic order along [111]. (b) Splitting into phonon modes with eigenfrequencies  $\omega_{\parallel}$  and  $\omega_{\perp}$ . (c) Nearest-neighbor coupling  $J_1$  and dominant next-nearest neighbor coupling  $J_2$ . (d) Néel temperatures vs  $J_2 S(S+1)$  using values for  $J_2$  taken from Ref. [26] in comparison to the mean-field expectation (dashed line).

deviations from the cubic symmetry in the magnetically ordered state were estimated in the case of MnO and NiO to be less than 1% of the phonon eigenfrequencies [6,27], while the exchange-driven and experimentally observed splittings are 1 order of magnitude larger [28–30].

In the case of the spinel systems  $ACr_2O_4$  with nonmagnetic ions  $A = Zn, Mg, Cd$ , the magnetic properties are determined by  $Cr^{3+}$  ions with spin  $S = 3/2$  in octahedral environment. The Cr sites form a pyrochlore lattice which can be regarded as a network of corner-sharing tetrahedra [see Figs. 2(a) and 2(b)]. The inherent frustration of Heisenberg spins on the pyrochlore lattice with antiferromagnetic nn exchange interaction  $J_{nn}$  can be lifted by taking into account nnn exchange coupling  $J_{nnn}$  [see Fig. 2(b)] [31] or magneto-elastic coupling leading to spin-Jahn-Teller transitions [2], which occur at Néel temperatures of 12.5, 12.7, and 7.8 K for  $ZnCr_2O_4$ ,  $MgCr_2O_4$ , and  $CdCr_2O_4$ , respectively [32,33]. These Néel temperatures are low in comparison to their Curie-Weiss temperatures of  $-390$ ,  $-346$ , and  $-71$  K [11,34] and, in contrast to the TMMOs, cannot be described in mean-field approximation using the dominant nn direct exchange constants  $J_{nn} = 1.44, 1.48$ , and  $0.63$  meV obtained from the analysis of the paramagnetic susceptibilities [see Fig. 2(c)] [30,35]. In the paramagnetic phase the four expected triply degenerate optical phonons are observable in the far infrared spectra for all three compounds [36]. For  $ZnCr_2O_4$  and  $CdCr_2O_4$  one of these modes reportedly exhibits a pronounced splitting into a singly and a doubly degenerate mode at  $T_N$  [11–13,15], analogously to the TMMOs.

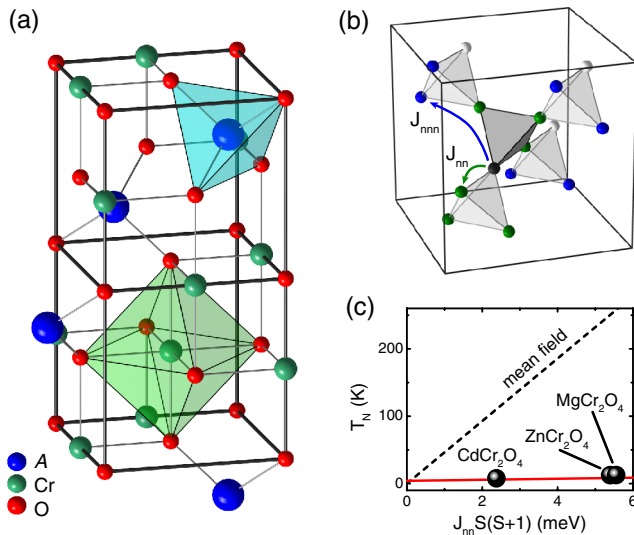


FIG. 2 (color online). (a) Cubic spinel structure of  $ACr_2O_4$ . Nonmagnetic  $A$ -site ions are in tetrahedral and the Cr ions in octahedral environment. (b) Nearest-neighbor and effective further nearest-neighbor exchange paths of the Cr ions on the pyrochlore lattice [30,31]. (c) Néel temperatures vs  $J_{nn}S(S+1)$  using values for  $J_{nn}$  taken from Ref. [30] in comparison to the mean-field expectation (dashed line).

Although the exact lattice symmetry and the spin configuration of the magnetically ordered state are still subject of debate [8,15,37,38], the dominant structural feature of the low-temperature phase is a tetragonal distortion with an elongation along [001] for  $CdCr_2O_4$  and a contraction for  $ZnCr_2O_4$  [33] and  $MgCr_2O_4$  [39].

The  $MgCr_2O_4$  single crystals were grown for this study by chemical transport in similar conditions as reported previously for  $ZnCr_2O_4$  [15]. Details for sample preparation and characterization of the other samples have been given earlier [15,40]. The magnetic susceptibilities of our spinel samples [30] agree nicely to the ones of fully stoichiometric samples [41]. In Fig. 3 we show the dielectric loss functions derived via the Kramers-Kronig relation from optical reflectivity spectra, of the transverse optical (TO) modes for the TMMOs [(a)–(d)] [23,29,40] and the

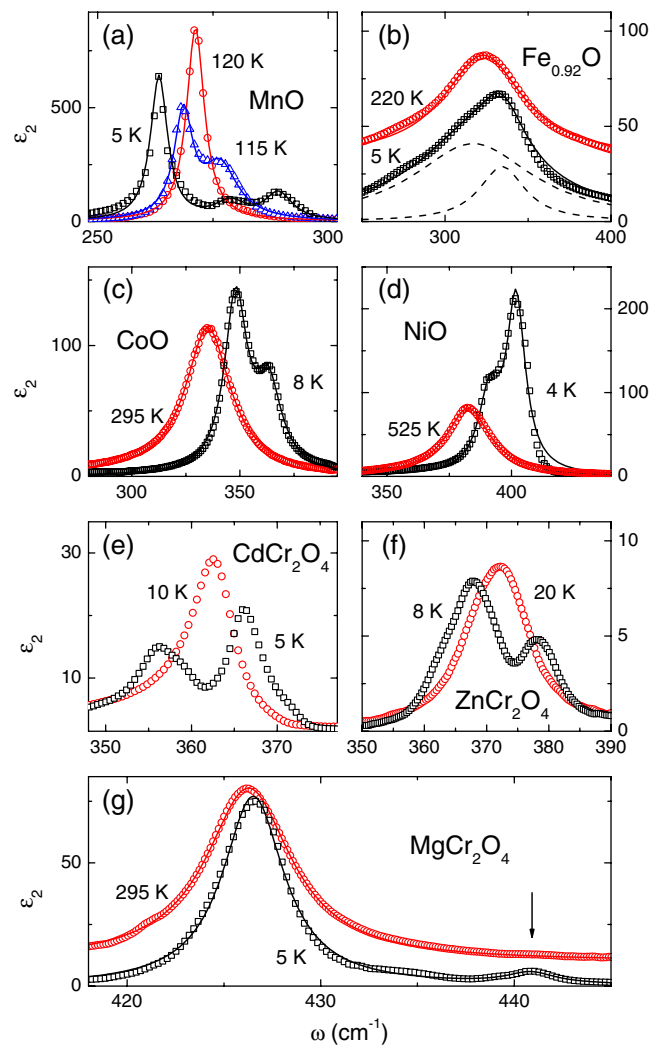


FIG. 3 (color online). Dielectric loss of (a) MnO, (b)  $Fe_{0.92}O$ , (c) CoO, (d) NiO, (e)  $CdCr_2O_4$ , (f)  $ZnCr_2O_4$ , and (g)  $MgCr_2O_4$  around the TO phonon modes above and below,  $T_N$  respectively. The high temperature data of  $Fe_{0.92}O$  and  $MgCr_2O_4$  are shifted upward for clarity. Lines indicate fits to the loss peaks (see text).

relevant phonon for the Cr spinels [(e)–(g)] [15] below and above the corresponding transition temperatures.

The splitting of the phonon mode is prominent in MnO [Fig. 3(a)] where above the Néel temperature ( $T_N = 118$  K [20]) one single Lorentzian-like normal mode can be detected. On cooling it splits right at the onset of long-range magnetic order, where a clear shoulder appears at 115 K. Finally, at 5 K three distinct oscillators can be identified. The overall splitting amounts to  $\Delta\omega = 25.6$   $\text{cm}^{-1}$ , which is in excellent agreement with neutron scattering results [28]. This splitting of approximately 10% of the cubic phonon frequency is 1 order of magnitude larger than what is expected from the structural distortions [6]. A similar analysis was performed for the other monoxides  $\text{Fe}_{0.92}\text{O}$ , CoO, and NiO. The corresponding dielectric loss functions at low temperatures and above  $T_N$  are plotted in Fig. 3(b)–3(d), respectively. In the paramagnetic state all spectra can be well described by a single symmetric Lorentzian line as indicated in the figure. At the onset of magnetic order a clear anisotropy becomes apparent in all compounds and at least two Lorentz oscillators are needed to describe the low-temperature phonon behavior. In the iron monoxide the split phonon modes appear as an asymmetric loss peak below  $T_N$  as depicted by the two dashed Lorentzian lines in Fig. 3(b), which were superposed to describe the spectrum. The origin of the comparatively broad peaks in  $\text{Fe}_{0.92}\text{O}$  may be due to strong anharmonicities and disorder in the iron deficient structure. At the lowest measured temperatures the overall splitting  $\Delta\omega$  can be evaluated from the peak maxima of the loss functions and amounts to 17.9  $\text{cm}^{-1}$ , 14.9  $\text{cm}^{-1}$ , and  $-10.3$   $\text{cm}^{-1}$  in  $\text{Fe}_{0.92}\text{O}$ , CoO, and NiO, respectively. The negative sign of  $\Delta\omega$  for NiO indicates that  $\omega_{\parallel} < \omega_{\perp}$  in agreement with a recent inelastic x-ray study reporting a splitting of  $-7.2$   $\text{cm}^{-1}$  at room temperature [27].

Figures 3(e)–3(g) present the respective results obtained for the chromium spinels. The case of  $\text{CdCr}_2\text{O}_4$  resembles the one of NiO, because the observed splitting  $\Delta\omega = -10$   $\text{cm}^{-1}$  of the cubic phonon mode [Fig. 3(e)] leads to  $\omega_{\parallel} < \omega_{\perp}$  [13,15], while for  $\text{ZnCr}_2\text{O}_4$  [Fig. 3(f)] and  $\text{MgCr}_2\text{O}_4$  [Fig. 3(g)] we encounter the opposite situation, with  $\Delta\omega = 11$   $\text{cm}^{-1}$  [11,15] and  $\Delta\omega = 14.3$   $\text{cm}^{-1}$ , respectively. The size of the splitting has previously been associated with the spin-phonon coupling effects due to the dominant direct nn exchange coupling  $J_{nn}$  of the  $\text{Cr}^{3+}$  ions residing on the frustrated pyrochlore lattice. The sign reversal of  $\Delta\omega$  in the case of  $\text{CdCr}_2\text{O}_4$  with respect to (Zn, Mg) $\text{Cr}_2\text{O}_4$ , however, could not be explained by this approach. It has been pointed out that this sign reversal is in contradiction to what is expected considering that in  $\text{CdCr}_2\text{O}_4$  the lattice undergoes an elongation along the tetragonal  $c$  axis (leading to  $\Delta\omega > 0$ ) while in  $\text{ZnCr}_2\text{O}_4$  and  $\text{MgCr}_2\text{O}_4$  it becomes contracted (leading to  $\Delta\omega < 0$ ) [13]. Hence, we face two scenarios, a purely structurally

driven splitting and a splitting due to spin-phonon coupling via the direct exchange coupling  $J_{nn}$ , but none of the two can explain the experimental observations for the phonon splitting in the Cr spinels.

Recently, Luo and co-workers [42] proposed for the TMMOs that the actual size of the exchange-driven phonon splitting  $\Delta\omega = \omega_{\parallel} - \omega_{\perp}$  is solely determined in sign and magnitude by the nondominant nn exchange  $J_1$  via  $\hbar\Delta\omega = \beta J_1 S^2$ , while the contributions of the dominant  $180^\circ$  nnn superexchange coupling  $J_2$  are canceled. Here,  $S$  denotes the spin of the transition-metal ion and  $\beta$  a dimensionless factor taking into account the dependence on lattice parameters and the vibrational displacements [42]. To test this prediction, we used quantitative theoretical estimates of  $J_1$  which have been obtained only recently [26]. Using these values we plot in Fig. 4 the experimentally observed splitting  $\Delta\omega$  against the expected exchange-induced splitting  $J_1 S^2$  for all investigated TMMOs. The linear dependence of both quantities evidences that not only the size of the splitting can be successfully described in the framework of the purely exchange-driven scenario, but even the sign change from an antiferromagnetic nn exchange in CoO to a ferromagnetic nn exchange in NiO is reflected by the inversion of the split phonon doublet and singlet modes. From a linear fit we obtain the dimensionless slope  $\beta = 3.7$ .

We extended this approach to the case of the Cr spinels. The nondominant nnn exchange constants  $J_{nnn} = 0.19$ , 0.25, and  $-0.17$  meV were obtained by the aforementioned analysis of the paramagnetic susceptibilities for  $\text{ZnCr}_2\text{O}_4$ ,  $\text{MgCr}_2\text{O}_4$ , and  $\text{CdCr}_2\text{O}_4$ , respectively [30]. Plotting the observed phonon splittings as a function of  $J_{nnn} S^2$ , we found a perfect correlation with the respective data on TMMOs in Fig. 4. Note that  $\text{CdCr}_2\text{O}_4$  differs from the other two Cr

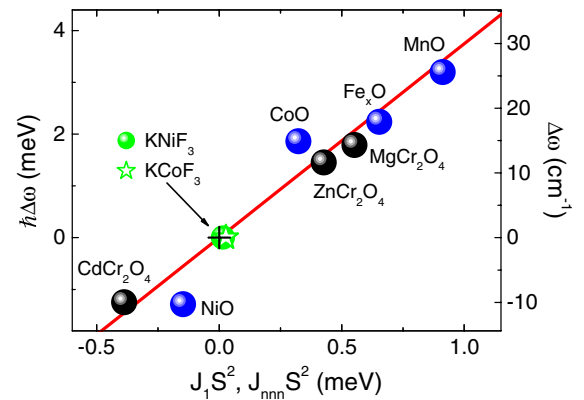


FIG. 4 (color online). Phonon splitting  $\hbar\Delta\omega$  vs nondominant exchange contributions  $J_1 S^2$  and  $J_{nnn} S^2$  for the investigated TMMOs and Cr spinels. The solid line is a linear fit to the experimental data of the TMMOs. The values for  $J_1$  and  $J_{nnn}$  are taken from Refs. [26,30], respectively. Values for the perovskite fluorides were taken from Refs. [48,49].

compounds by the reversed sign of  $J_{\text{nnn}}$  (indicating an effective nondominant ferromagnetic coupling similar to NiO), although the absolute values of  $J_{\text{nnn}}$  are comparable for all three spinel compounds. The agreement between the sign change of the nondominant exchange constant and the inversion of the split modes may resolve the dilemma to match the observed lattice distortion and the phonon splitting in  $\text{CdCr}_2\text{O}_4$  mentioned above. Indeed, this finding suggests to look at spin-phonon splitting in highly frustrated magnets from a new perspective and challenges the prevailing approach to attribute the phonon splitting to the effects of the dominating exchange interaction [11,12].

Moreover, we find not only a linear relation for the spinels, too, but even a perfect match with the line with slope  $\beta = 3.7$  obtained for the TMMOs. This result indicates that the phonon splitting in both classes of materials originates from the same underlying mechanism, namely, the exchange-driven splitting determined *in size and sign* by the nondominant exchange coupling, yielding a universal proportionality factor of 3.7. A universal law will have the power to predict the nondominant exchange splitting, if the phonon splitting is known, and vice versa. A remarkable feature in this respect is that no exchange-induced phonon splitting is expected, if the nondominant coupling is negligible, because the universal line passes through the origin.

To comply with the situation in the TMMOs and the Cr spinels, further systems ought to be cubic in the paramagnetic phase and only undergo a distortion when AFM ordering sets in. Moreover, this scenario should be valid for materials of another different structural class. We identified corresponding materials in the class of transition-metal perovskites, namely  $\text{KCoF}_3$  and  $\text{KNiF}_3$  with corresponding Neel temperatures of 114 and 275 K [43], respectively. Most AFM perovskites are prone to show deviations from cubic symmetry already above the Néel temperature, but in  $\text{KNiF}_3$  no deviations from cubic symmetry could be resolved even below  $T_N$  while cubic  $\text{KCoF}_3$  undergoes a small tetragonal distortion in the AFM state [43]. Moreover, the above systems are considered paradigmatic isotropic Heisenberg antiferromagnets with negligible nnn exchange coupling [44–47]. In addition, optical IR studies of these two compounds did not resolve any splitting of the three cubic triply degenerate IR active modes below  $T_N$  [48,49]. Adding the data for this class of cubic AFM perovskites to Fig. 4 is clearly consistent with the universal line derived from the rock-salt and spinel type antiferromagnets and further supports our finding. Further materials such as, for example, CrN [50] or MnSe [51] should be reexamined with respect to an exchange-induced phonon splitting.

Although the linear slope has been predicted in a straightforward manner for the TMMOs in [42], a detailed analysis of direct and indirect exchange interactions and

their dependence on the respective phonon-modulated exchange paths of all three classes of antiferromagnets appears to be necessary [52]. In particular, the role of nondominant couplings has not been treated in previous theoretical approaches [6,12], and Uchiyama suggested that charge-transfer processes and Jahn-Teller effects play an important role in the TMMOs [53]. In this respect we would like to point out three routes, which could provide further insight into the observed phenomenological relation: (i) calculations similar to the ones performed for the TMMOs [6] and the spinels [12], where the exchange-driven phonon splitting was assumed to stem from the dominant exchange coupling, should be undertaken for the perovskite systems, too. (ii) Experimentally, it might be possible to move along the universal curve by changing the size of the nondominant exchange coupling by an external parameter (such as pressure or magnetic field), to determine this change and track down the respective phonon splitting in the optical experiment. The pressure dependence of the exchange coupling constants has been predicted for the TMMOs [26]. The nondominant coupling will increase under pressure and, e.g., in MnO one may expect a significantly enhanced phonon splitting under hydrostatic pressure for the universal line. (iii) Finally, we want to mention that the influence of pressure on the Néel temperature and magnetic excitations has previously been studied for some TMMOs and led to the empirical law  $-\partial \ln J / \partial \ln V \simeq 10/3$  for the volume dependence of superexchange interactions [54,55].

In summary, we found a universal linear relation of the observed splitting of the zone-center optical phonon and the nondominant exchange couplings in transition-metal monoxides and frustrated Cr-oxide spinels, yielding a dimensionless slope of 3.7. For the TMMOs our results are in agreement with the predictions for an exchange-driven phonon splitting by the nondominant nn exchange coupling. The universal linear relation not only correctly describes the size of the splitting, but even the sign change in the nondominant exchange coupling is compatible with the inversion of the phonon modes with eigenfrequencies  $\omega_{\parallel}$  and  $\omega_{\perp}$ . In systems with negligible nondominant coupling such as the perovskites  $\text{KCoF}_3$  and  $\text{KNiF}_3$  the universal law predicts no splitting in agreement with the experimental observation. This paves a new way for understanding spin-phonon coupling effects in antiferromagnets and, in particular, their role in releasing frustration in highly frustrated magnets.

It is a pleasure to thank Walt Harrison and H. Uchiyama for stimulating discussions and a critical reading of the manuscript, and we acknowledge fruitful discussions with F. Rivadulla, C. Batista, G.-W. Chern, and O. Tschernyshyov. This work was supported by the Deutsche Forschungsgemeinschaft via TRR 80 (Augsburg-Munich) and project DE 1762/2-1.

- \*Corresponding author.  
joachim.deisenhofer@physik.uni-augsburg.de
- [1] Y. Yamashita and K. Ueda, *Phys. Rev. Lett.* **85**, 4960 (2000).
- [2] O. Tchernyshyov, R. Moessner, and S.L. Sondhi, *Phys. Rev. Lett.* **88**, 067203 (2002).
- [3] A. Pimenov, A.A. Mukhin, V.Y. Ivanov, V.D. Travkin, A.M. Balbashov, and A. Loidl, *Nature Phys.* **2**, 97 (2006).
- [4] H. Katsura, A.V. Balatsky, and N. Nagaosa, *Phys. Rev. Lett.* **98**, 027203 (2007).
- [5] G. Lawes, T. Kimura, C. Varma, M. Subramanian, R. Cava, and A. Ramirez, *12th US-Japan Seminar on Dielectric and Piezoelectric Ceramics: Annapolis, Nov. 6-9*, (2005).
- [6] S. Massidda, M. Posternak, A. Baldereschi, and R. Resta, *Phys. Rev. Lett.* **82**, 430 (1999).
- [7] S.-H. Lee, C. Broholm, W. Ratcli, G. Gasparovic, Q. Huang, T.H. Kim, and S.-W. Cheong, *Nature (London)* **418**, 856 (2002).
- [8] J.-H. Chung, M. Matsuda, S.-H. Lee, K. Kakurai, H. Ueda, T.J. Sato, H. Takagi, K.-P. Hong, and S. Park, *Phys. Rev. Lett.* **95**, 247204 (2005).
- [9] K. Tomiyasu, H. Suzuki, M. Toki, S. Itoh, M. Matsuura, N. Aso, and K. Yamada, *Phys. Rev. Lett.* **101**, 177401 (2008).
- [10] V. Tsurkan, S. Zherlitsyn, V. Felea, S. Yasin, Y. Skourski, J. Deisenhofer, H.-A.K. von Nidda, P. Lemmens, J. Wosnitza, and A. Loidl, *Phys. Rev. Lett.* **106**, 247202 (2011).
- [11] A.B. Sushkov, O. Tchernyshyov, W. Ratcliff II, S.W. Cheong, and H.D. Drew, *Phys. Rev. Lett.* **94**, 137202 (2005).
- [12] C.J. Fennie and K.M. Rabe, *Phys. Rev. Lett.* **96**, 205505 (2006).
- [13] R.V. Aguilar, A.B. Sushkov, Y.J. Choi, S.-W. Cheong, and H.D. Drew, *Phys. Rev. B* **77**, 092412 (2008).
- [14] T. Rudolf, C. Kant, F. Mayr, M. Schmidt, V. Tsurkan, J. Deisenhofer, and A. Loidl, *Eur. Phys. J. B* **68**, 153 (2009).
- [15] C. Kant, J. Deisenhofer, T. Rudolf, F. Mayr, F. Schrettle, A. Loidl, V. Gnezdilov, D. Wulferding, P. Lemmens, and V. Tsurkan, *Phys. Rev. B* **80**, 214417 (2009).
- [16] J. Kuneš, A. V. Lukoyanov, V.I. Anisimov, R. T. Scalettar, and W.E. Pickett, *Nature Mater.* **7**, 198 (2008).
- [17] J. Zaanen, G.A. Sawatzky, and J.W. Allen, *Phys. Rev. Lett.* **55**, 418 (1985).
- [18] P.W. Anderson, *Phys. Rev.* **79**, 350 (1950).
- [19] W.L. Roth, *Phys. Rev.* **110**, 1333 (1958).
- [20] B. Morosin, *Phys. Rev. B* **1**, 236 (1970).
- [21] C.A. McCammon and L.-g. Liu, *Phys. Chem. Miner.* **10**, 106 (1984).
- [22] F. Schrettle, Ch. Kant, P. Lunkenheimer, F. Mayr, J. Deisenhofer, and A. Loidl, [*Eur. Phys. J. B* (to be published)].
- [23] C. Kant, T. Rudolf, F. Schrettle, F. Mayr, J. Deisenhofer, P. Lunkenheimer, M. V. Eremin, and A. Loidl, *Phys. Rev. B* **78**, 245103 (2008).
- [24] C. Henry La Blanchetais, *J. Phys. Radium* **12**, 765 (1951).
- [25] H.P. Rooksby, *Nature (London)* **152**, 304 (1943).
- [26] G. Fischer, M. Däne, A. Ernst, P. Bruno, M. Lüders, Z. Szotek, W. Temmerman, and W. Hergert, *Phys. Rev. B* **80**, 014408 (2009).
- [27] H. Uchiyama, S. Tsutsui, and A. Q. R. Baron, *Phys. Rev. B* **81**, 241103 (2010).
- [28] E.M.L. Chung, D.M. Paul, G. Balakrishnan, M.R. Lees, A. Ivanov, and M. Yethiraj, *Phys. Rev. B* **68**, 140406(R) (2003).
- [29] T. Rudolf, C. Kant, F. Mayr, and A. Loidl, *Phys. Rev. B* **77**, 024421 (2008).
- [30] C. Kant, J. Deisenhofer, V. Tsurkan, and A. Loidl, *J. Phys. Conf. Ser.* **200**, 032032 (2010).
- [31] G.-W. Chern, R. Moessner, and O. Tchernyshyov, *Phys. Rev. B* **78**, 144418 (2008).
- [32] M.T. Rovers, P.P. Kyriakou, H.A. Dabkowska, G.M. Luke, M.I. Larkin, and A.T. Savici, *Phys. Rev. B* **66**, 174434 (2002).
- [33] S.-H. Lee, C. Broholm, T.H. Kim, W. Ratcli II, and S.-W. Cheong, *Phys. Rev. Lett.* **84**, 3718 (2000).
- [34] T. Rudolf, C. Kant, F. Mayr, J. Hemberger, V. Tsurkan, and A. Loidl, *Phys. Rev. B* **75**, 052410 (2007).
- [35] A.J. García-Adeva and D.L. Huber, *Phys. Rev. Lett.* **85**, 4598 (2000).
- [36] H.D. Lutz, B. Müller, and H.J. Steiner, *J. Solid State Chem.* **90**, 54 (1991).
- [37] S.-H. Lee, G. Gasparovic, C. Broholm, M. Matsuda, J.-H. Chung, Y.J. Kim, H. Ueda, G. Xu, P. Zschack, K. Kakurai, H. Takagi, W. Ratcli, T.H. Kim, and S.-W. Cheong, *J. Phys. Condens. Matter* **19**, 145259 (2007).
- [38] S. Ji, S.-H. Lee, C. Broholm, T.Y. Koo, W. Ratcli, S.-W. Cheong, and P. Zschack, *Phys. Rev. Lett.* **103**, 037201 (2009).
- [39] H. Ehrenberg, M. Knapp, C. Baetz, and S. Klemme, *Powder Diffr.* **17**, 230 (2002).
- [40] C. Kant, F. Mayr, T. Rudolf, M. Schmidt, F. Schrettle, J. Deisenhofer, and A. Loidl, *Eur. Phys. J. Special Topics* **180**, 43 (2010).
- [41] S.E. Dutton, Q. Huang, O. Tchernyshyov, C.L. Broholm, and R.J. Cava, *Phys. Rev. B* **83**, 064407 (2011).
- [42] W. Luo, P. Zhang, and M.L. Cohen, *Solid State Commun.* **142**, 504 (2007).
- [43] A. Okazaki and Y. Suemune, *J. Phys. Soc. Jpn.* **16**, 671 (1961).
- [44] L.J. de Jongh and A.R. Miedema, *Adv. Phys.* **23**, 1 (1974).
- [45] H. Yamaguchi, K. Katsumata, M. Hagiwara, and M. Tokunaga, *Phys. Rev. B* **59**, 6021 (1999).
- [46] M.E. Lines, *Phys. Rev.* **164**, 736 (1967).
- [47] W.J.L. Buyers, T.M. Holden, E.C. Svesson, R.A. Cowley, and M.T. Hutchings, *J. Phys. C* **4**, 2139 (1971).
- [48] J.D. Axe and G.D. Pettit, *Phys. Rev.* **157**, 435 (1967).
- [49] M. Balkanski, P. Moch, and M.K. Teng, *J. Chem. Phys.* **46**, 1621 (1967).
- [50] A. Filippetti and N.A. Hill, *Phys. Rev. Lett.* **85**, 5166 (2000).
- [51] Z. Popovic and A. Milutinovic, *Phys. Rev. B* **73**, 155203 (2006).
- [52] W.A. Harrison, *Phys. Rev. B* **76**, 054417 (2007).
- [53] H. Uchiyama, *Phys. Rev. B* **85**, 014419 (2012).
- [54] D. Bloch, *J. Phys. Chem. Solids* **27**, 881 (1966).
- [55] K.C. Johnson and A.J. Sievers, *Phys. Rev. B* **10**, 1027 (1974).